JOURNAL OF Materials CHEMISTRY

Identification of superconducting phases in the Ba–Ca–Cu–O system: an unstable phase with $T_c \approx 126$ K and its derivative with $T_c \approx 90$ K

T. Hosomi,[a,b] H. Suematsu,[a] H. Fjellvåg,[c] M. Karppinen[a,d] and H. Yamauchi[a,b]

[a]*Materials and Structures Laboratory, Tokyo Institute of Technology, Yokohama 226–8503, Japan. E-mail: yamauchi@materia.titech.ac.jp*
[b]*Department of Innovative and Engineered Materials, Tokyo Institute of Technology, Yokohama 226–8502, Japan*
[c]*Department of Chemistry, University of Oslo, N-0315 Oslo, Norway*
[d]*Laboratory of Inorganic and Analytical Chemistry, Helsinki University of Technology, FIN-02015 Espoo, Finland*

Received 3rd November 1998, Accepted 11th February 1999

Superconducting samples with T_c values as high as 126 K were obtained in the Ba–Ca–Cu–O system by means of high-pressure synthesis. The X-ray powder diffraction pattern obtained for the as-synthesized 126 K phase was indexed with a tetragonal unit cell and lattice parameters, $a = 3.85$ Å and $c = 28.3$ Å. When exposed to air, the 126 K phase changes to another superconducting phase with $T_c \approx 90$ K. The crystal structure of the 90 K derivative phase was successfully studied by electron and synchrotron X-ray powder diffraction. The unit cell has body-centered symmetry, space group $I4/mmm$, $a = 3.8486$ Å, $c = 33.979$ Å. The metal composition in the 90 K phase was estimated by EDX to be Ba : Ca : Cu = 2.0 : 2.1 : 3, and from TG-MS and IR spectroscopy analyses the presence of H_2O molecules (and possibly also carbonate groups) was revealed. A layered-cuprate M-*m*223 structure was concluded for each of the two phases. For the 90 K phase, two types of structural models, assuming either H or (H,C) composition for the charge-reservoir constituent M, were derived and tested. However, refinement of the synchrotron diffraction data could not differentiate between the two models, both giving reasonable agreement with experimental data. For the 126 K phase, a 0223 structure is proposed, and the location of the oxygen atom in the $(BaO)_2$ double layer is discussed. Finally, it is believed that, upon the phase change, besides H_2O (CO_2) molecules, additional protons from a redox reaction involving copper and/or peroxide-type oxygen are incorporated into the 126 K phase.

The structures of superconducting cuprates are built up from a continuous piling of $M_mO_{m\pm\delta}$ perovskite or rock-salt blocks (*i.e.* 'charge-reservoir' block), AO rock-salt planes and $Q_{n-1}Cu_nO_{2n}$ perovskite blocks (*i.e.* 'infinite-layer' block), and are best described as members of different homologous series expressed by $M_mA_2Q_{n-1}Cu_nO_{m+2+2n\pm\delta}$ or M-*m*2(*n*−1)*n*.[1,2] This notation includes also the '02(*n*−1)*n*' series comprising the phases in which no $M_mO_{m\pm\delta}$ charge-reservoir block is found but the $Q_{n-1}Cu_nO_{2n}$ infinite-layer blocks are separated by a double $(AO)_2$ layer only. The first 02(*n*−1)*n* series was discovered in the Sr–Ca–Cu–O system in 1993 when high-pressures (≈5 GPa) were applied for the synthesis.[3,4] The highest T_c in this series, obtained for the $n = 3$ member, is 109 K.[4,5] In 1994, in an attempt to totally replace Sr by Ba in the 02(*n*−1)*n* phases of the Sr–Ca–Cu–O system, a new homologous series, *i.e.* Cu-12(*n*−1)*n* : P (P stands for a perovskite-type charge-reservoir block), with Cu as the charge-reservoir constituent M was discovered in the Ba–Ca–Cu–O system.[6–9] [Note that, empirically it is established that $M_mA_2Q_{n-1}Cu_nO_{m+2+2n\pm\delta}$ phases with A = Ba show higher T_c values than corresponding phases with A = Sr.] Later it was found that part of the copper atoms in the charge reservoir can be replaced by carbonate groups without affecting the T_c value considerably.[10] The $n = 3$ member in the (Cu,C)-12(*n*−1)*n* series possesses a T_c as high as ≈120 K.[11] Recently, Nunez-Regueiro *et al.*[12] reported indications of even higher T_c (a kink in the dc susceptibility curve at 126 K) in the Ba–Ca–Cu–O system, and Chu *et al.*[13,14] obtained, *via* high-pressure synthesis, multi-phase Ba–Ca–Cu–O samples showing a sharp superconducting transition at 126 K.

The new Ba–Ca–Cu–O phase with $T_c \approx 126$ K was considered by Chu *et al.*[13,14] to be non-stoichiometric with a composition of $(Ca_xCu_y)Ba_2Ca_2Cu_3O_{8+\delta}$, $0.4 \leqslant x \leqslant 0.9$ and $0 \leqslant y \leqslant 0.7$, *i.e.* with interstitial Ca_x, Cu_y and O_δ randomly inserted between two adjacent BaO planes in the charge-reservoir block. [Although Chu *et al.*[15] termed the phase '0223', their structure model does not correspond to a 0223 structure. If their model was right, the phase should rather be called '(Ca,Cu)-1223 : H', since the portion of 'the charge-reservoir block plus the two BaO planes' is of a Cu_2AlMn (Heusler alloy)-type structure, consisting of (Ca,Cu), O and Ba atoms.[16] [Note also that the space group of a (Ca,Cu)-1223 : H phase is of body-centered (*I*) symmetry.] The structure analysis by Xue *et al.*[14] was based on X-ray powder diffraction and showed a tetragonal unit cell with body-centered symmetry and lattice constants, $a = 3.84$ Å and $c = 28.2$ Å. However, the exact structure remained unsolved due to the phase instability and multi-phase character of all samples which contained this novel high-T_c phase. In humid air, the as-synthesized phase with $T_c \approx 126$ K rapidly degrades to a lower-T_c phase. The lower-T_c phase which shows superconductivity only up to ≈90 K has an expanded lattice constant $c \approx 33.8$ Å. A composition of $(Ca,Cu,H,CO_2)_2Ba_2Ca_2Cu_3O_{8+\delta}$ corresponding to the (Ca,Cu,H,C)-2223 structure (of *I* symmetry) was proposed for the $T_c \approx 90$ K phase.[14] Also, a related Ca-1223 phase [of primitive (*P*) symmetry] with $T_c \approx 107$ K was recently stabilized by Wu *et al.*[17] using a high-pressure synthesis technique.

In the present contribution, the more precise chemical compositions and crystal structures of the new 126 K phase and its derivative phase with $T_c \approx 90$ K in the Ba–Ca–Cu–(H–C–)O system are concerned. Both phases were analyzed by X-ray diffraction (XRD) and superconducting quantum interference device (SQUID) measurements. The change in air of the higher-T_c phase to the lower-T_c phase was followed in repeated XRD and SQUID measurements. Further, the gas evolution upon thermal treatment of the

samples was analyzed by means of combined thermogravimetric and mass spectroscopic (TG-MS) techniques, and the chemical environments of carbon and hydrogen in the samples were probed by infrared (IR) absorption spectroscopy. Due to the instability of the as-synthesized phase, only the 90 K derivative phase could be characterized in more detail with respect to composition and crystal structure, *i.e.* by high-resolution transmission electron microscopy (HR-TEM) and electron diffraction (ED) analysis for crystal symmetry, by energy dispersive X-ray (EDX) analysis for chemical composition and by synchrotron X-ray powder diffraction for precise structure determination.

Experimental

Starting materials for the high-pressure syntheses were $BaCuO_{2+\delta}$, Ca_2CuO_3 and $Ba_2Cu_3O_{5+\delta}$ together with AgO which was added to act as an 'external oxygen source'. [An 'external oxygen source' oxide such as AgO should release oxygen upon high-pressure application, and the cation of the oxide is supposed not to be included in the reaction product.[18]] The $BaCuO_{2+\delta}$, Ca_2CuO_3 and $Ba_2Cu_3O_{5+\delta}$ precursors were first prepared by repeated heat treatments under the following conditions: (i) $BaCuO_{2+\delta}$ from BaO_2 and CuO powders at 850 °C in flowing O_2 gas for 40 h with one intermediate pulverization, (ii) Ca_2CuO_3 from $CaCO_3$ and CuO powders at 950 °C in flowing O_2 gas for 40 h with one intermediate pulverization, and (iii) $Ba_2Cu_3O_{5+\delta}$ from BaO_2 and CuO powders at 620 °C in flowing O_2 gas for 12 h. The amounts of excess oxygen in the two Ba–Cu precursors were determined *via* chemical titrations. [Note that both $BaCuO_{2+\delta}$ and $Ba_2Cu_3O_{5+\delta}$ are also supposed to act as 'internal oxygen sources' during the high-pressure synthesis.[18]] When using $BaCuO_{2+\delta}$ as a barium source, the precursors were mixed into a cationic molar ratio of Ba : Ca : Cu = 2 : 2 : 3, whereas in the case of $Ba_2Cu_3O_{5+\delta}$ a Cu-rich ratio of 2 : 2 : 4 was used. The amount of AgO was varied between 0 and 200 mol% (relative to the amount of desired cuprate). All operations, such as mixing and compaction of the powders, were carried out in a glove bag filled with dry N_2 gas to avoid humidity and contamination by carbon. The precursor mixtures were sealed in gold capsules. Each capsule was covered with a NaCl separator and a graphite heater, and loaded into a cubic pyrophyllite cell, the medium of pressure. The cubic cell was placed into a cubic-anvil-type high-pressure apparatus, and the precursor mixture was allowed to react at 5 GPa and 770 °C for 30 min, before being quenched to room temperature.

The superconducting properties of the obtained samples were characterized using a SQUID magnetometer (Quantum Design, MPMS-5S) with an applied magnetic field of 10 Oe at temperatures between 5 and 130 K. The obtained T_c values are onset temperatures of the (diamagnetic) Meissner signal. After the superconducting properties had been measured for the bulk samples, the sample pellets were crushed and the phase contents were analyzed by XRD (MAC Science, MXP18VAHF[22]; CuKα radiation). In order to collect an XRD pattern for the 126 K phase before its phase change, the as-synthesized samples were placed in a sample chamber where dry N_2 gas was introduced. The phase evolution process was studied during repeated SQUID and XRD measurements.

For HR-TEM experiments crushed powders were suspended in CCl_4 using an ultrasound homogenizer, scooped on carbon microgrids that were supported by molybdenum meshes and then dried. Thin wedges of the powders were selected for TEM observations. Crystallographic structures were studied utilizing a TE microscope (Hitachi H-1500) operated at an accelerating voltage of 800 kV. Chemical compositions were studied by an EDX spectroscope (NORAN Inst., VOYAGER III) which was attached to a TE microscope (JEOL, JEM-2010FEF) operated at an accelerating voltage of 200 kV. For quantitative chemical analysis, EDX spectra were collected for the $BaCuO_{2+\delta}$ and Ca_2CuO_3 precursors with the same grids, sample holder and geometry as those used for the superconducting samples in order to deduce k factors (Cliff–Lorimer factors).

Gaseous decomposition products released from the samples during heat treatment were analyzed by a mass spectrometer (MS; VG, PC300D) attached to a thermogravimetric apparatus (TG; MAC Science, TG-DTA 2000S). Bulk samples were heated at a constant heating rate of 20 °C min^{-1} from room temperature to 1000 °C in flowing He gas. The released gases were introduced to the spectrometer and the mass numbers 18 (H_2O), 32 (O_2) and 48 (CO_2) were detected. In order to establish the decomposition temperatures more exactly, independent TG measurements were done for parallel samples with a slower heating rate of 2 °C min^{-1} in the same temperature range. In the TG and TG-MS experiments the sample mass was 10–70 mg.

Infrared absorption spectra were recorded for the 126 K phase (as-synthesized sample in bulk form) and 90 K phase (in powder form) samples and for the $BaCO_3$ reference (in powder form) in the range of 400–4000 cm^{-1} by an IR spectroscopic analyzer (BIO RAD, WIN-IR PRO FTS 6000) with an additional photoacoustic spectroscopy attachment (IR-PAS; CIR-PA). All the measurements were performed in a sample chamber filled with dry N_2 gas in order to both prevent the phase change in the as-synthesized sample and avoid IR absorption of CO_2 and H_2O gases contained in air.

Synchrotron X-ray powder diffraction data were collected for the 90 K phase at the Swiss–Norwegian Beam Line, European Synchrotron Radiation Facility (ESRF), Grenoble, in order to deduce more detailed information on the crystal structure. Photons with wavelength 0.69978 Å were obtained from a Si(111) channel cut monochromator. Diffraction data were collected between $2\theta = 10°$ and 52° in steps of 0.012°. The crystal structure was refined according to the Rietveld method[19] using a program named GSAS.[20] Five hundred and ninety Bragg reflections (from Ba–Ca–Cu–O and four impurity phases) contributed to the observed profile with 3455 data points. The background was described as a 15 term cosine Fourier series, and the rather broad reflections by a pseudo-Voigt peak-shape function (including the GSAS parameter ptec). In the refinements, soft distance restraints were imposed upon C–O (1.25 ± 0.01 Å), Ca–O (2.48 ± 0.03 Å) and Ba–O (2.75 ± 0.05 Å) bonding separations (see below).

Results and discussion

Synthesis of the 126 K phase and its change in air to the 90 K phase

Superconducting samples with $T_c \approx 126$ K were reproducibly obtained from the high-pressure synthesis under the conditions of 5 GPa and 770 °C using either $BaCuO_{2+\delta}$ or $Ba_2Cu_3O_{5+\delta}$ as the barium source. When using $BaCuO_{2+\delta}$, more AgO (100–200 mol%) was needed than in the case of the $Ba_2Cu_3O_{5+\delta}$ precursor (0–50 mol%). This fact is consistent with chemical analysis which shows that the $Ba_2Cu_3O_{5+\delta}$ precursor ($\delta \approx 0.7$) is more oxidized than the $BaCuO_{2+\delta}$ precursor ($\delta \approx 0.1$). The main Bragg reflections in the X-ray powder diffraction pattern obtained for the as-synthesized sample correspond to the 126 K phase. However, all the high-pressure synthesis products obtained were multiphased, the impurities being BaO_2, CuO, a high-pressure form of Ag_2O and some unknown high-pressure phase(s).

The 126 K phase was found to be unstable in open air at room temperature, in accordance with previous reports by Xue *et al.*[14,17,21] After exposure of the as-synthesized sample to air for 45 min at room temperature, new peaks were seen in the XRD pattern, and a shoulder appeared in the susceptibil-

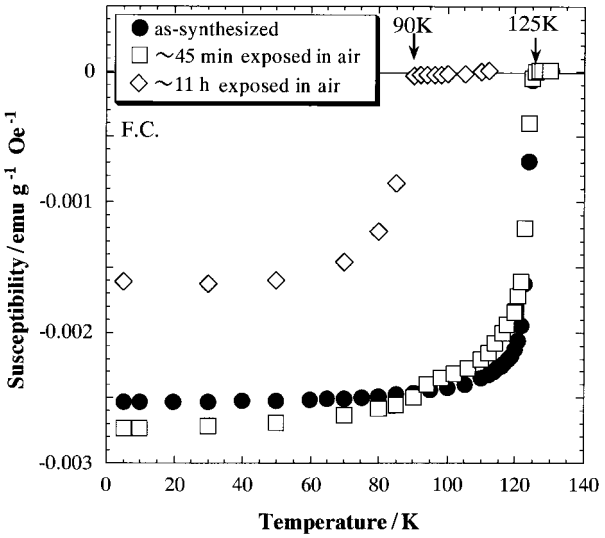

Fig. 1 Magnetic susceptibility data for an as-synthesized 126 K phase sample, and for the same sample after partial and complete conversions on exposure to air at room temperature.

ity curve around 90 K (Fig. 1). After 11 hours exposure to air at room temperature, no sign of the 126 K phase could be seen anymore in the susceptibility curve. Instead a bulk superconductivity transition was found at 90 K. In the XRD pattern obtained for the $T_c \approx 90$ K sample, dominant peaks for the 126 K phase were absent whereas new sharp peaks appeared.

ED and HR-TEM observations and EDX analysis of the 90 K phase

In Fig. 2, the [010] electron diffraction pattern obtained for the 90 K phase is shown. The systematic extinctions observed for diffraction spots in the ED pattern suggest body-centered symmetry (Table 1). The spots correspond to the main reflections seen in the XRD pattern for lattice constants $a = 3.85$ Å and $c = 33.9$ Å. If one assumes the 126 K phase to have the same symmetry, almost all main reflections in the XRD pattern can be indexed with $a = 3.85$ Å and $c = 28.3$ Å.

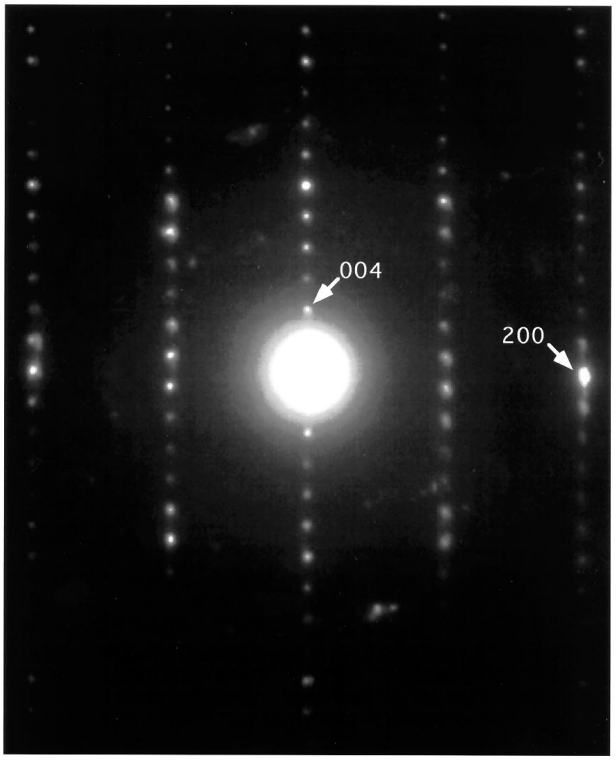

Fig. 2 Electron diffracton pattern for the 90 K phase viewed along [010].

Table 1 Extinguished reflections and possible space groups for the Ba–Ca–Cu–O superconducting phase with $T_c = 90$ K

Incident beam	Extinguished reflections	Conditions	Possible space groups
Electron	$h0l$	$h+l=$ odd	
	$h00$	$h=$ odd	$I4$, $I\bar{4}$, $I4/m$*, $I422$,
	$00l$	$l=$ odd	$I4mm$, $I\bar{4}m2$, $I42m$,
X-ray	hkl	$h+k+l=$ odd	$I4/mmm$*
	$hk0$	$h+k=$ odd	

Fig. 3 presents the HR-TEM image obtained for a grain which had first been confirmed by ED to be the 90 K phase. The image reveals a periodical structure with parallel bright rows at an interval of about 16.6 Å. These bright rows inevitably represent the charge-reservoir block. Nevertheless, the 2D-Fourier transform of the HR-TEM image shows P symmetry for the phase, and the c axis length is slightly shorter than the $c/2$ value refined from the XRD data for the 90 K phase of I symmetry. The change in symmetry and the contraction of the c axis with the subjection of the sample to electron-beam irradiation are believed to be due to evaporation of some (light) elements from the charge-reservoir block. Actually, even from the ED pattern, development of some additional weak diffraction spots can be deduced.

Even though the charge-reservoir block of the 90 K phase gradually changes when the sample is subjected to electron-beam irradiation, the infinite-layer block is supposed to remain quite unaffected. In the HR-TEM image of Fig. 3, the dark lines seen on both sides of the bright rows represent the heaviest atoms in the crystal, *i.e.* Ba of the BaO rock-salt layers. The observed distance of about 10.8 Å between two separate BaO layers over the infinite-layer block is suitable for accommodating three CuO_2 planes separated from each other by a calcium layer [*i.e.* $n=3$ in M-$m2(n-1)n$]. On the other hand, the distance between two adjacent BaO layers over the charge-reservoir block in the 90 K phase can be estimated as 6.15 Å from the thickness of the infinite-layer block observed by HR-TEM and from the $c/2$ length obtained by XRD. This distance is longer than the charge-reservoir thickness reported for (Cu,C)-1234 (4.38 Å[22]) and Hg-1223 (5.54 Å[23]), but shorter than that of Tl-2223 (7.53 Å[24]). In other words, the charge-reservoir block of the 90 K phase is thicker than those of the known M-$12(n-1)n$ type structures. According to Xue *et al.*,[14] the charge-reservoir block of the 90 K phase is filled with (Cu,Ca,C,H,O) atoms, but no details of the structure were reported. In the present HR-TEM study, the charge-

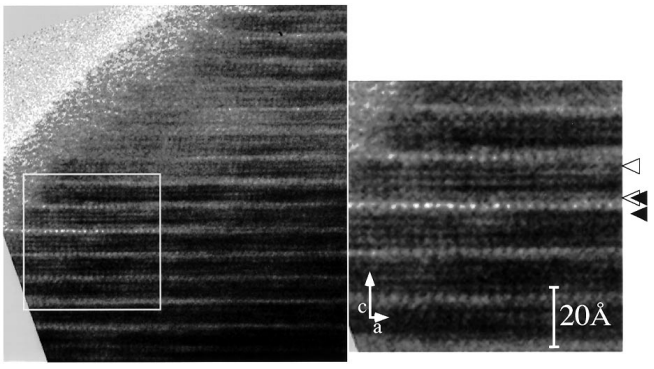

Fig. 3 HR-TEM image of the *ac* plane of the 90 K phase. In the partial enlargement, the filled triangles indicate two nearest BaO layers sandwiching a bright row, and the open triangles indicate two BaO layers sandwiching an infinite-layer block.

reservoir block was found to consist of very light element(s) only, probably with small atomic size. Therefore the number, *m*, of MO layers in the charge-reservoir block may be quite large.

Quantitative EDX analysis was carried out for the grain confirmed by ED and HR-TEM to be the 90 K phase. The EDX analysis clearly revealed a metal composition Ba : Ca : Cu = 2.0 : 2.1 : 3, *i.e.* the phase corresponds to an M-*m*223 structure with only light element(s) in the charge-reservoir block. Since the metal composition is believed to remain unchanged upon room-temperature conversion of the 126 K phase into the 90 K phase, the *m*223 composition is expected for the 126 K phase as well. [Note that no Ag was detected in the grain, confirming that AgO did not enter the superconducting phase but worked purely as an oxygen source.]

TG-MS analysis of the 126 K and 90 K phases

In order to gain further information on the chemical composition of the 126 K and 90 K phases with respect to light elements in their charge-reservoir blocks, the decomposition characteristics and the gaseous products evolved upon heat treatment in inert atmosphere (He or Ar) were investigated by TG-MS and TG experiments. Two samples were prepared for the TG-MS analysis. According to SQUID measurements, the '126 K phase sample' contained 8 vol% of the 126 K phase. The '90 K phase sample' was obtained by opening a capsule which initially contained 23 vol% of the 126 K phase two days before the TG-MS analysis. This period was sufficient to convert the 126 K phase to the 90 K phase completely. The TG-MS runs were carried out in He atmosphere with a constant heating rate of 20 °C min^{-1}. The high heating rate was chosen to ensure detectable signals for the evolved gases in the MS analysis. However, in non-isothermal thermoanalytical experiments application of high heating rates shifts all signals (both TG and MS) to higher temperatures as compared to corresponding equilibrium temperature values. Therefore, additional TG experiments were carried out in Ar atmosphere with a low heating rate of 2 °C min^{-1}, to be able to estimate the equilibrium decomposition temperatures as well.

The TG-MS profiles obtained for the two samples are shown in Fig. 4. During the heat treatments in He atmosphere up to 1000 °C release of O_2, H_2O, and CO_2 gases was detected for both samples. The evolution of O_2, H_2O and CO_2 seen for the samples below ≈350 °C with smoothly decreasing intensity with increasing temperature was attributed to adsorbed gases on the sample and/or on the equipment wall. The most prominent feature believed to be related to the decomposition of the 90 K phase is the intense and distinct evolution of H_2O seen below 520 °C in Fig. 4(b). On the basis of several parallel TG-MS and TG experiments it was confirmed that the MS signal and the corresponding weight loss in the TG curve are characteristic of samples containing the 90 K phase. In the TG-MS profile recorded for the 126 K phase sample [Fig. 4(a)], only a very small H_2O signal (probably due to minor amounts of the 90 K phase, formed after opening the capsule for the TG-MS experiment) is seen below 520 °C. This strongly suggests that the phase change occurring on ageing of the as-synthesized 126 K phase in air is accompanied by incorporation of H_2O. From additional TG experiments carried out in Ar for several aged samples at a heating rate of 2 °C min^{-1}, the equilibrium temperature for evolution of H_2O from the 90 K phase was estimated as ≈260 °C. The relatively high decomposition temperature, as well as the sharpness of the corresponding MS peak, suggest that the H and O atoms are bound by rather strong and uniform chemical bonds in the crystal structure of the 90 K phase. The amount of H_2O released from the 90 K phase could be roughly estimated from

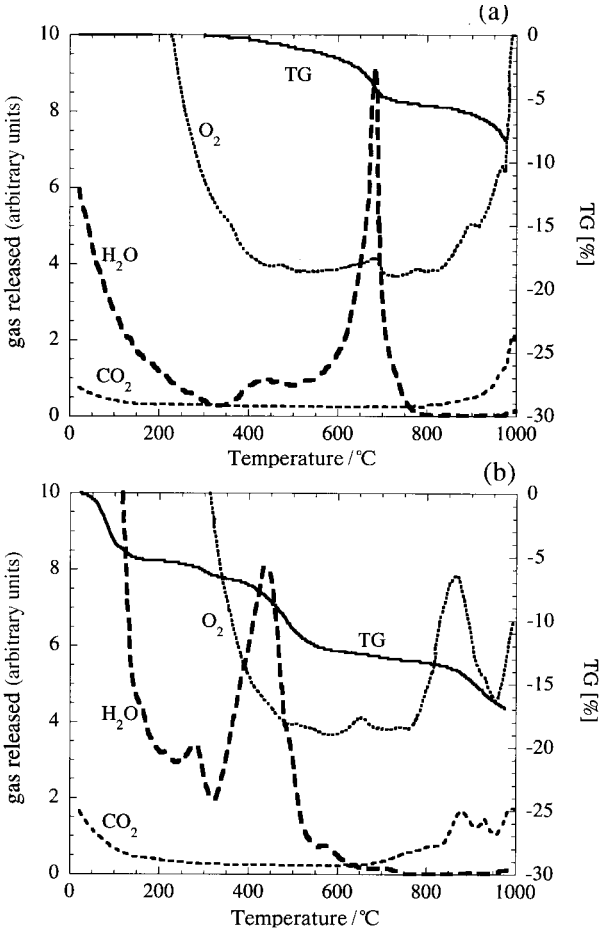

Fig. 4 TG-MS profiles for (a) an as-synthesized sample with 8 vol% of the 126 K phase, and (b) a sample of the 90 K phase, formed from a sample with 23 vol% of the 126 K phase. The sample masses were 68.8 mg and 72.7 mg, respectively. The heating rate was 20 °C min^{-1} in 1 atm He.

the weight losses observed in several parallel TG runs. Taking an estimation for the phase content (≈60 mass%) obtained for the superconducting phase from XRD measurements into account, around 2.5–3 H_2O molecules per charge-reservoir unit are deduced.

Since no CO_2 was evolved from the 90 K phase simultaneously with the H_2O molecules, see Fig. 4(b), a straightforward conclusion would be that the 90 K phase does not contain carbonate. However, a critical question to be answered is, why should an M-*m*223 phase containing both H and C atoms in the charge-reservoir block decompose in a single step with simultaneous release of H_2O and CO_2? Actually, no definite reason can be given. On the other hand, it appears improbable that a possible intermediate decomposition product of C-*m*223 would remain stable at temperatures considerably higher than the decomposition temperature of the related high-pressure synthesized (Cu,C)-1223 phase (in the same Ba–Ca–Cu–C–O system). The (Cu,C)-1223 phase was found to decompose to simple and binary compounds around 400 °C in Ar.[11,25] In the present TG-MS profile of the 90 K phase sample [Fig. 4(b)], evolution of CO_2 is seen only above 700 °C. [The corresponding equilibrium onset temperature for the CO_2 evolution is around 550–600 °C.] It is possible that the carbon, which is evolved above 700 °C from the sample, is originally from the superconducting 90 K phase. But it could also stem from some Ba-containing impurity phase, which was in the form of hydroxide in the as-synthesized material [*cf.* the H_2O evolution around 700 °C in Fig. 4(a)] but converted into carbonate or oxycarbonate during the two-day exposure in air, to yield the CO_2 evolution peak(s) seen

above 700 °C in Fig. 4(b). Consistently with this explanation, no sign of H_2O evolution around 700 °C is seen in the TG-MS profile of Fig. 4(b). With the available analysis techniques no definite conclusion on the existence or absence of carbon in the 90 K phase can be given. Anyhow, the present TG-MS results suggest that the carbon content in the 90 K phase is quite low compared with the hydrogen content. [If all the CO_2 molecules released from the 90 K phase sample below 1000 °C were assigned to the 90 K phase, the amount would be around 1–1.5 CO_2 molecules per charge-reservoir unit.] The 90 K phase must hence be expressed either as H-*m*223 or as (H,C)-*m*223.

Finally, it should be noted that the small H_2O evolution peak seen in Fig. 4(b) below 300 °C is most probably due to some impurity phase, since it was detected only in one single sample out of several 90 K phase samples studied. The evolution of O_2 around 650 °C for both the 126 K and 90 K phase samples (Fig. 4) is assigned to release of excess oxygen from oxygen-rich Ba-containing impurities such as BaO_2, $Ba_{1-y}CuO_{2+\delta}$ and $Ba_2Cu_3O_{5+\delta}$.

Infrared absorption analysis of the 126 K and 90 K phases

The chemical environments of the H and C atoms in the 126 K and 90 K phase samples were investigated by means of IR-PAS absorption spectroscopy. The spectra were recorded in the range of 400–4000 cm^{-1} from the following two superconducting samples: an as-synthesized 126 K phase sample in bulk form (with a superconducting volume fraction of 22 vol%) and an aged 90 K phase sample in powder form (with a superconducting volume fraction of 15 vol%). A spectrum of $BaCO_3$ powder was measured for a reference. The intensity of the spectrum obtained for the 126 K phase sample was very low over the whole wavenumber range measured, probably due to the small surface area of the bulk sample. However, a weak but distinguishable absorption peak, which may be attributed to a carbonate group, was seen around 1400 cm^{-1}. On the other hand, in the 90 K phase sample the existence of carbonate groups was evident. The splitting of the carbonate peaks in the 90 K phase sample was very similar to that seen in the $BaCO_3$ reference sample, suggesting that the carbonate is bonded in the same way in these two structures. In $BaCO_3$, the carbonate group is almost planar and regular with quite a constant C–O bond length of 1.286 Å and all the three oxygen atoms bonded also to barium.[26] The fact that the carbonate vibrations in the 90 K phase sample are very similar to those in $BaCO_3$ suggests that the carbonate groups seen in the 90 K phase sample are mainly from $BaCO_3$ impurity. The same may be said for the 126 K phase sample, though the very low peak intensity makes interpretation difficult.

The most characteristic feature in the absorption spectrum of the 90 K phase sample was a broad peak at 2700–3700 cm^{-1}. This peak is typically found in inorganic materials containing crystal water.[27] Since this peak is lacking in the spectrum of the 126 K phase sample, it can be assigned to the 90 K phase rather than to some impurity phase in the sample. The broadness of this –OH vibration peak indicates that there are different O–H bond strengths in the structure.

Structure models for the 126 K and 90 K phases

Calcium and barium atoms empirically favor different sites in an $M_mA_2Q_{n-1}Cu_nO_{m+2+2n\pm\delta}$ structure. Calcium tends to be in the infinite-layer block (*i.e.* Q atom), whereas barium occupies the cation site in the rock-salt layer (*i.e.* A atom). It is therefore very likely that the structure of the 90 K phase which according to EDX analysis has a metal atom stoichiometry of Ba : Ca : Cu = 2.0 : 2.1 : 3 accommodates three CuO_2 layers in its infinite-layer block. This is furthermore fully consistent with the HR-TEM data described earlier. The structure of the 90 K phase is thus represented by a layer

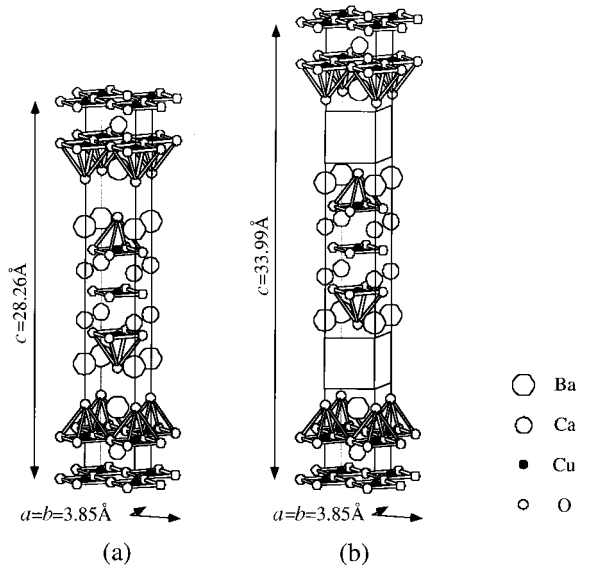

Fig. 5 Proposed structure models for (a) the 126 K phase and (b) the 90 K phase.

sequence –[charge-reservoir block]–(BaO)–[(CuO_2)–(Ca)–(CuO_2)–(Ca)–(CuO_2)]– (BaO)–, see Fig. 5. In the $M_mA_2Q_{n-1}Cu_nO_{m+2+2n\pm\delta}$ cuprates, the $M_mO_{m\pm\delta}$ charge-reservoir block determines the crystal symmetry. Body-centered symmetry is typically found for the $02(n-1)n$ and $22(n-1)n$ phases. In general, *I* symmetry is expected for the M-$m2(n-1)n$ phases with $m=2l$ ($l=0$, 1, 2...) when the charge-reservoir block is of either rock-salt or perovskite type structure.

For the charge-reservoir block in the 90 K phase, TG-MS analysis shows the presence of H and O atoms. However, the actual atomic arrangement can not be directly verified by the available analysis techniques, but probable models can be suggested on the basis of analogous structure elements in inorganic compounds and tested with respect to the measured diffraction data, see below. In case the block contains solely H and O, the ice structure with tetrahedrally coordinated oxygen is of relevance, with two covalent O–H bonds and two O···H hydrogen bonds. Some possible structural models for an (H,O)-charge-reservoir block of the 90 K phase are proposed in Fig. 6. In these models an even number of O layers is inserted in the charge-reservoir block and the number of H_2 layers is estimated as m = number of O layers + 1. This kind of structure can be expressed as H-*m*223 : I (I stands for an 'ice-type' charge reservoir), and the atomic arrangement is consistent with body-centered symmetry (even though *m* is an

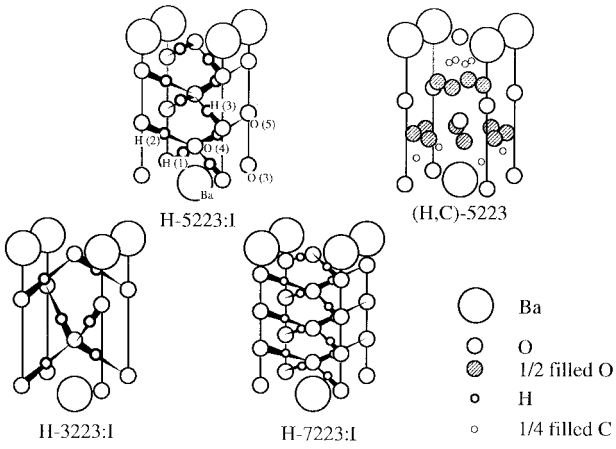

Fig. 6 Examples of structure models tested for the charge-reservoir block of the 90 K phase.

odd number). The existence of an ice-type structural arrangement being thermally stable up to around 260 °C does not seem very likely, however. If not, one has to consider inclusion of other light elements in the block, in particular carbon. It should be noted that certain material classes, like hydrotalcites, are stabilized strongly (entirely) by CO_3 groups in between 2-D layers. It may be possible that the 90 K phase is stabilized by carbonate, which subsequent to phase decomposition becomes bonded to barium as $BaCO_3$ or some other Ba compound and therefore partly escapes detection in the TG-MS analysis. In Fig. 6, a reasonable candidate model for a charge-reservoir structure containing both water and carbonate, *i.e.* (H,C)-5223, is shown.

In all known M-$m2(n-1)n$ superconducting cuprates the nominal charge of the $M_mO_{m\pm\delta}$ charge-reservoir block varies between 0 and +2, being close to +1 in the most well-established cases such as $Cu(III)O_{1-\delta}$, $Bi(III)_2O_{2+\delta}$, $Tl(III)_{1-x}O_{1-\delta}$, $Tl(III)_{2-x}O_{2-\delta}$ and $Hg(II)O_{1-\delta}$.[28] A higher nominal charge for the charge-reservoir block implies less oxidized CuO_2 planes in the infinite-layer block, and *vice versa*. Based on the result of EDX analysis and the fact that *I* symmetry was revealed from the XRD pattern, the structure of the 126 K phase is most likely of 0223. The $02(n-1)n$ structures are built up without any charge-reservoir block, *i.e.* the nominal charge of the charge reservoir can be considered to be zero. Consequently, if one supposes full occupancy of the apical oxygen site in the $(AO)_2$ rock-salt layers as well as perfect CuO_2 planes in the infinite-layer block, the $02(n-1)n$ structures should be much more oxidized in terms of nominal copper valence than other high-T_c superconducting cuprates.[28] For example, the average nominal copper valence in the 0223 structure would be as high as +2.66. Therefore, a possible driving force for the instability of the 0223 structure towards incorporation of additional molecules or ions in between AO planes could be the strive to reduce the 126 K phase. That is, the overall charge of the accommodated species should be positive. In the proposed H-$m223$:I models for the 90 K phase (Fig. 6), the charge-reservoir block consists of m hydrogen planes with two H atoms and $(m-1)$ oxygen planes with one O atom, leading to a chemical composition $H_{2m}O_{m-1}$ and a nominal charge of +2 for the charge-reservoir block. In this case incorporation of water in the 0223 structure is connected with a redox reaction

$$4\ Cu(III) + 2\ H_2O \rightarrow 4\ Cu(II) + O_2 + 4\ H^+ \qquad (1)$$

and additional incorporation of protons. Such a mechanism would equally well apply for the (H,C)-5223 model.

For the 0223 structure of the 126 K phase, the interlayer distance between the CuO_2 plane and the Ba layer is estimated as ≈2.0 Å. This is based on comparison between the observed and simulated XRD patterns. In the observed XRD pattern no peaks around $2\theta \approx 32.1°$ were seen, while in the simulated pattern substantial intensity appears for the (107) reflection at $2\theta \approx 32.1°$ when the CuO_2–Ba interlayer distance exceeds 2.0 Å. Furthermore, a rough description of the crystal structure can be constructed (Fig. 7) supposing that the interlayer distance between the CuO_2 planes (Cu–Cu distance) in the infinite-layer block is 3.15 Å, a value typically observed for M-$m223$ phases. Taking the c-axis length ($c/2 = 14.15$ Å) obtained for the 126 K phase by XRD into account, an interlayer distance of 3.85 Å between the two adjacent Ba layers over the 'zero' charge reservoir is deduced. In order to understand the special characteristics related to the high nominal oxidation state of the $02(n-1)n$ phases in the Ba–Ca–Cu–O system, the location of the oxygen atom in the $(BaO)_2$ double layer, *i.e.* apical oxygen for the Cu atom in the CuO_2 plane, should be refined. The location can not be directly extracted from the X-ray powder diffraction data but an interesting clue for the position may be obtained by considering the bond-valence-sum rule around the Ba atom.[29] For 9-coordinated Ba, an average Ba–O bond length of 2.81 Å would satisfy the rule. With the interlayer distance of 2.0 Å between the CuO_2 plane and the Ba layer, and an a-axis parameter of 3.85 Å, the four Ba–O bonds from Ba to the CuO_2-plane oxygen atom would be slightly shorter (*i.e.* ≈2.78 Å) than the average length. Therefore the other five Ba–O bonds should be somewhat longer, *i.e.* ≈2.87 Å on average. This would place the oxygen atom in the $(BaO)_2$ double layer ≈0.9 Å out of the Ba plane. In other words, in the $(BaO)_2$ double layer oxygen would be sandwiched in between two Ba planes rather than being located in an ideal rock-salt position, see Fig. 7. In this kind of Ba–O_2–Ba block, oxygen atoms might even tend to cluster into peroxide-type O_2^{2-} pairs, providing one possible explanation for the high nominal oxidation state of the $02(n-1)n$ phases. In order to experimentally justify the proposed structure model for the 126 K phase, a neutron powder diffraction study has been initiated.

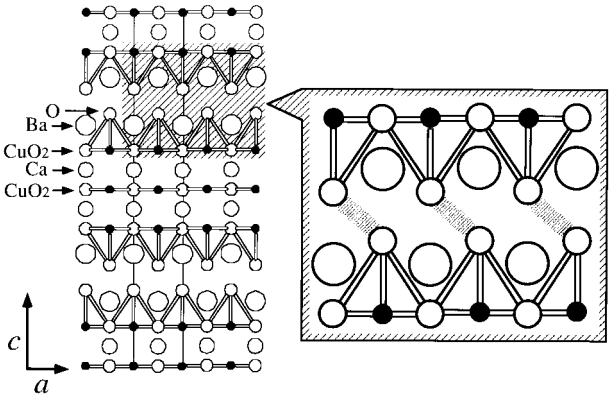

Fig. 7 Possible structure model for the charge-reservoir block of the 126 K phase.

Refinement of the structure of the 90 K phase on the basis of synchrotron X-ray powder diffraction data

The 90 K phase sample studied by synchrotron XRD contained at least four impurities, *i.e.* the high-pressure form of Ag_2O, CuO, BaO_2 (all included in the refinements) and unidentified high-pressure phase(s). In order to reduce the contributions from the latter phases, six smaller scattering regions were excluded from the refinements.

Two types of structural models were derived and tested. The first model type, *i.e.* H-$m223$:I, assumes that the charge-reservoir block is filled with O and H (water and protons). Several variants of this type were tested. The second main model, *i.e.* (H,C)-5223, assumes filling up by O, C and H (carbon dioxide, water and protons). In both cases the positional parameters were refined for all atoms, except the H atoms. The large content of heavily scattering atoms in Ba–Ca–Cu–O makes the location of the light elements in the charge reservoir impossible by means of X-ray photons. For some of the H-$m223$:I models, the positional parameters for the O atoms in the charge-reservoir block were fixed in order to give equal distances between adjacent layers. For refinement of the (H,C)-5223 model, all positional parameters were refined; however, strong distance restraints were included for the light element units (*i.e.* C–O, and assumed hydrogen bonded O–H···O). Both models have interatomic distances which must be considered as acceptable for hydrates and/or carbonates.

The obtained *R*-factors for the refinements must be considered as equivalent for the H-$m223$:I and (H,C)-5223 models. Hence, it is not possible from diffraction data alone to differentiate between these models. Convergence was obtained for the H-5223:I and (H,C)-5223 models, in both cases with conventional *R* factors: $R_{wp} = 10.81\%$ and $R_p =$

Table 2 Atomic coordinates, occupancy, and thermal parameters for the 90 K phase as derived from Rietveld refinement of synchrotron X-ray data. Calculated standard deviations in parentheses. Space group *I*4/*mmm*, unit cell dimensions $a=3.8486(4)$ Å, $c=33.979(4)$ Å

Atom	*x*	*y*	*z*	Occupancy	B/Å^2
(A) H-5223 : I structure					
Cu(1)	0	0	0	1.0	0.4(1)
Cu(2)	0	0	0.0922(3)	1.0	0.4(1)
Ca	0.5	0.5	0.0486(3)	1.0	0.4(1)
Ba	0.5	0.5	0.1537(2)	1.0	2.3(2)
O(1)	0.5	0.0	0	1.0	1.6(4)
O(2)	0.5	0	0.0949(4)	1.0	1.6(4)
O(3)	0	0	0.1645(12)	1.0	1.6(4)
O(4)	0.5	0.5	0.2332(9)	0.5	2.5
O(5)	0.0	0.0	0.2299(46)	0.5	2.5
H(1)	0.25	0.25	0.18330	0.5	2.5
H(2)	0.25	0.25	0.21667	0.5	2.5
H(3)	0.25	0.25	0.25	0.5	2.5
(B) (H,C)-5223 structure					
Cu(1)	0	0	0	1.0	0.4(1)
Cu(2)	0	0	0.0910(2)	1.0	0.4(1)
Ca	0.5	0.5	0.0487(3)	1.0	0.4(1)
Ba	0.5	0.5	0.1545(1)	1.0	2.3(2)
O(1)	0.5	0.0	0	1.0	2.6(4)
O(2)	0.5	0	0.0950(4)	1.0	2.6(4)
O(3)	0	0	0.1557(8)	1.0	2.6(4)
C	0.600(1)	0.600(1)	0.6889(13)	0.25	2.0
O(4)	0.5	0.215(2)	0.2828(8)	0.5	2.0
O(5)	0	0	0.7341(7)	1.0	2.0

8.50%. The refined unit cell dimensions, positional, thermal and occupancy parameters are given for both models in Table 2 and corresponding bond lengths are collected in Table 3. For the *z* coordinates of the Cu(2) and O(2) atoms, one would expect that $z[\mathrm{Cu}(2)]>z[\mathrm{O}(2)]$; however, the unconstrained refinements for both models gave the opposite situation. The difference in *z* coordinates is very minor, however. Additional refinements under the constraint $z[\mathrm{Cu}(2)]=z[\mathrm{O}(2)]$ gave only slightly larger reliability factors. Most probably any deviation from a square-planar Cu(2)–O(2) arrangement is insignificant. Refinements based on the H-3223 : I and H-7223 : I structure models shown in Fig. 6 were also performed, however, the fit was somewhat poorer.

The H-*m*223 : I models have structure elements corresponding to that of ice. It seems not very likely that the oxide should incorporate water molecules and build an ice-like structure which is quite temperature stable. On that basis, the (H,C)-5223 model appears more likely. Barium oxide(s) has a strong tendency towards carbonatization reactions, and it is not to be excluded that such reactions may take place at ambient conditions. In certain layered materials, like the (Mg,Al)-hydrotalcites, CO_2 is incorporated between layers at very mild conditions.

Conclusions

Superconducting samples with T_c values as high as 126 K were obtained in the Ba–Ca–Cu–O system from Ca_2CuO_3 and $BaCuO_{2+\delta}/Ba_2Cu_3O_{5+\delta}$ precursors in a reproducible way under an ultra-high pressure (5 GPa) but at a relatively low temperature (770 °C). The X-ray powder diffraction pattern obtained for the as-synthesized 126 K phase was indexed with a tetragonal unit cell and lattice parameters, $a=3.85$ Å and $c=28.3$ Å. When subjected to air, the 126 K phase changed to another superconducting phase with $T_c=90$ K. The crystal symmetry and lattice parameters of the 90 K derivative phase were successfully deduced from electron and synchrotron X-ray powder diffraction data. The unit cell has body-centered symmetry, space group *I*4/*mmm*, $a=3.8486$ Å, $c=33.979$ Å. HR–TEM observations and microscopic-area chemical analysis by TEM-EDX revealed that the 90 K phase accommodates three CuO_2 planes in a unit structure with a metal composition of $\mathrm{Ba:Ca:Cu}=2:2:3$. The same metal composition was assumed for the 126 K phase. Consequently, a layered M-*m*223 structure was proposed for the both phases.

The distance between two BaO layers over the charge-reservoir block, *i.e.* the thickness of the charge-reservoir block, estimated for the 90 K phase ($\approx$6.15 Å) is longer than the charge-reservoir thickness reported for M-12($n-1$)n type structures (4.3–5.6 Å) but shorter than that of Tl-2223 ($\approx$7.5 Å). From TG-MS and IR spectroscopy analyses the presence of H_2O molecules (and possibly also carbonate groups) in the 90 K phase was concluded. Therefore, two types of structural models, assuming either H or (H,C) composition for the charge-reservoir constituent M, were derived and tested. Both models, having five light-element cation layers in the charge-reservoir block, gave a reasonable agreement with the experimental synchrotron X-ray diffraction data, however, refinement of the data could not differentiate these models.

For the 126 K phase, a 0223 structure, with a Ba–Ba distance over the 'zero' charge-reservoir block roughly estimated as $\approx$3.85 Å, is proposed. With this long Ba-Ba distance, it might be possible that the oxygen atom would be located in between the two Ba layers rather than in the ideal rock-salt position. A possible driving force for the instability of the 0223 structure towards incorporation of molecules and/or ions in between BaO planes could be the strive to reduce the highly oxidized phase. It is believed that, upon the phase change, additional protons from a redox reaction involving copper and/or peroxide-type oxygen are incorporated in the 'zero' charge-reservoir block of the 126 K phase.

Table 3 Selected interatomic distances [Å] for the H-5223 : I and (H,C)-5223 structures

Bond	H-5223 : I	(H,C)-5223
Cu(1)–O(1)	1.924(2)	1.924(2)
Cu(2)–O(2)	1.927(1)	1.929(1)
Cu(2)–O(3)	2.46(4)	2.20(3)
Ca–O(1)	2.536(6)	2.537(6)
Ca–O(2)	2.486(8)	2.486(8)
Ba–O(2)	2.774(10)	2.792(10)
Ba–O(3)	2.746(5)	2.722(19)
Ba–O(4)	2.700(31)	2.988(18)
Ba–O(5)	—	2.704(26)

Acknowledgements

The authors are indebted to Mr. K. Tojima of MAC Science Ltd. for his group's assistance in TG-MS measurements. They are also grateful to Prof. Y. Tomokiyo of Kyushu University and Dr. Y. Matsui of NIRIM for their help in TEM observations, and to Prof. N. Yamamoto of Tokyo Institute of Technology for his suggestions in interpreting the HR-TEM images. The help provided by Mr. K. Kameshima, Prof. Okada and Prof. T. Seki of Tokyo Institute of Technology in IR spectroscopic measurements is gratefully acknowledged.

The synchrotron study was enabled by the Contribution No 98.13 from the Swiss–Norwegian Beam Line at ESRF. The skillful assistance by Dr. K. Knudsen and Dr. P. Pattison is gratefully acknowledged.

This work was supported by a Grant-in-Aid for Scientific Research of contract No. 08044135 from The Ministry of Education, Science and Culture of Japan, and also by an International Collaborative Research Project Grant-1998 of the Materials and Structures Laboratory, Tokyo Institute of Technology.

References

1 H. Yamauchi, M. Karppinen and S. Tanaka, *Physica C*, 1996, **263**, 146.

2 H. Yamauchi and M. Karppinen, *Superlatt. Microstruct*., 1997, **21A**, 127.
3 S. Adachi, H. Yamauchi, S. Tanaka and N. Mori, *Physica C*, 1993, **208**, 226.
4 S. Adachi, H. Yamauchi, S. Tanaka and N. Mori, *Physica C*, 1993, **212**, 164.
5 T. Kawashima and E. Takayama-Muromachi, *Physica C*, 1996, **267**, 106.
6 C.-Q. Jin, S. Adachi, X.-J. Wu, H. Yamauchi and S. Tanaka, *Physica C*, 1994, **223**, 238.
7 X.-J. Wu, S. Adachi, C.-Q. Jin, H. Yamauchi and S. Tanaka, *Physica C*, 1994, **223**, 243.
8 M. A. Alario-Franco, C. Chaillout, J. J. Capponi, J. L. Tholence and B. Souleite, *Physica C*, 1994, **222**, 243.
9 H. Ihara, K. Tokiwa, H. Ozawa, M. Hirabayashi, A. Negishi, H. Matsuhara and Y. S. Song, *Jpn. J. Appl. Phys*., 1994, **33**, L503.
10 T. Kawashima, Y. Matsui and E. Takayama-Muromachi, *Physica C*, 1994, **224**, 69.
11 C. Chaillout, S. Le Floch, E. Gautier, P. Bordet, C. Acha, Y. Feng, A. Sulpice, J. L. Tholence and M. Marezio, *Physica C*, 1996, **266**, 215.
12 M. Nunez-Regueiro, M. Jaime, M. A. Alario-Franco, J. J. Capponi, C. Chaillout, J. L. Tholence, A. Sulpice and P. Lejay, *Physica C*, 1994, **235–240**, 2093.
13 C. W. Chu, Z. L. Du, Y. Cao, Y. Y. Xue, Y. Y. Sun, I. Ruskova and L. Gao, *Philos. Mag. B*, 1997, **75**, 15.
14 Y. Y. Xue, Y. Y. Sun, I. A. Rusakova, D. K. Ross, Z. L. Du, N. L. Wu, Y. Cao, L. Gao, B. R. Hickey and C. W. Chu, *Physica C*, 1998, **294**, 316.
15 C. W. Chu, Y. Y. Xue, Z. L. Du, Y. Y. Su, L. Gao, N. L. Wu, Y. Cao, I. Rusakova and K. Ross, *Science*, 1997, **277**, 1081.
16 H. Yamauchi and T. Hosomi, *Chemistry* (*Kagaku*), 1998, **53**(6), 74 (in Japanese).
17 N. L. Wu, Z. L. Du, Y. Y. Xue, I. Rusakova, D. K. Ross, L. Gao, Y. Cao, Y. Y. Sun, C. W. Chu, M. Hervieu and B. Raveau, *Physica C*, 1998, in press.
18 T. Ito, H. Suematsu, H. Sakata, O. Fukunaga, M. Karppinen and H. Yamauchi, *Mater. Sci. Eng. B*, 1998, **54**, 112.
19 J. Rietveld, *J. Appl. Crystallogr*., 1969, **2**, 65.
20 A. C. Larson and R. B. von Dreele, GSAS General Structure Analysis System, LANSCE, MS-H 805, Los Alamos National Laboratory, Los Alamos, NM 87545, USA.
21 L. Gao, Z. L. Du, Y. Cao, I. Rusakova, Y. Y. Sun, Y. Y. Xue and C. W. Chu, *Mod. Phys. Lett. B*, 1995, **21**, 1397.
22 Y. Shimakawa, J. D. Jorgensen, D. G. Hinks, H. Shaked, R. L. Hitterman, F. Izumi, T. Kawashima, E. Takayama-Muromachi and T. Kamiyama, *Phys. Rev. B*, 1994, **50**, 16008.
23 L. W. Finger, R. M. Hazen, R. T. Downs, R. L. Meng and C. W. Chu, *Physica C*, 1994, **226**, 216.
24 D. E. Cox, *Phys. Rev. B*, 1998, **38**, 6624.
25 T. Ito, H. Suematsu, K. Isawa, M. Karppinen and H. Yamauchi, *Physica C*, 1998, **308**, 9.
26 J. P. R. de Villiers, *Am. Min*., 1971, **56**, 758.
27 R. A. Nyquist and R. O. Kagel, *Infrared Spectra of Inorganic Compounds* (3800–45 cm^{-1}), Academic Press, New York, 1971.
28 M. Karppinen and H. Yamauchi, *Philos. Mag. B*, 1999, **79**, 343.
29 I. D. Brown and D. Altermatt, *Acta Crystallogr.*, *Sect. B*, 1985, **41**, 244.

Paper 8/08546C